

# Hydromagnesite Rectangular Thin Sheets as Efficient Heterogeneous Catalysts for the Synthesis of 3-Substituted Indoles via Yonemitsu-Type Condensation in Water

U. Chinna Rajesh, V. Satya Pavan, and Diwan S. Rawat\*

Department of Chemistry, University of Delhi, Delhi 110007, India

## Supporting Information

**ABSTRACT:** The anisotropic controlled assembly of nano-building blocks into uncommon uniform rectangular thin sheet morphology of hydromagnesite (RS-HM) with a high surface area of 110 m<sup>2</sup>/g was achieved by a simple conventional heating under green reaction condition. The synthesized RS-HM was calcined at 450 °C in the presence of air and resulted in the formation of MgO with a surface area 120 m<sup>2</sup>/g. RS-HM was found to be a more efficient catalyst than MgO for the synthesis of novel 3-substituted indoles via Yonemitsu-type condensation selectively in excellent yields. The present method has advantages such as environmentally benign, ease to handle, selectivity and excellent yields, low *E*-factor (0.15) and high atom economy (96%).

**KEYWORDS:** Hydromagnesite, Reusable base catalyst, 3-Substituted indoles, Yonemitsu-type condensation, *E*-factor and atom economy



## INTRODUCTION

In recent years, the morphology controlled synthesis of nanomaterials has attracted the attention of the scientific community due to the applications in diverse fields.<sup>1,2</sup> The control over size and morphology of nanostructures to tailor the physical and chemical properties has played a significant role in activity and selectivity of nanocatalysts in organic conversions.<sup>3,4</sup> Moreover, nanocatalysis has advantages such as simple workup, ease of handling, reducing waste production, recovery and reuse of catalyst, thus aggrandizing green and sustainable chemistry.<sup>5</sup> The *E*-factor and atom economy concept has played a significant role in minimization of waste, which is usually generated from chemical industries during their manufacture processes.<sup>6</sup> Several solid base catalysts such as zeolites, metal oxides, mixed oxides and hydrotalcites have been developed for the manufacture of fine chemicals in heterogeneous systems.<sup>7</sup> Hydromagnesite [Mg<sub>5</sub>(CO<sub>3</sub>)<sub>4</sub>(OH)<sub>2</sub>·4H<sub>2</sub>O] is a precursor of MgO the presence of carbonate and hydroxide functionalities makes it similar to hydrotalcites.<sup>8,9</sup> The structure of hydromagnesite was determined as a three-dimensional framework of MgO<sub>6</sub> octahedra.<sup>10</sup> Hydromagnesite is widely used in plastic and rubber industries as fire retardants,<sup>11,12</sup> but its catalytic applications have not been well investigated.<sup>13,14</sup> Recently, we reported the flower-like sheet morphology of hydromagnesite as a solid base catalyst for organic conversions in water.<sup>15</sup> This opens up a new direction for further investigation on the synthesis of a more efficient morphology of hydromagnesite with a high surface

area. The three-dimensional structural model of hydromagnesite has been generated using Schrodinger material suite software, as shown in Figure 1.

In 1978, Yonemitsu et al. reported the one-pot three component reaction using indoles, aldehydes and Meldrum's acid for the synthesis of 3-substituted indole derivatives.<sup>16</sup> Since then, the Yonemitsu reaction has attracted attention of synthetic chemists due to its wide applications for the construction of biologically active molecules.<sup>17</sup> However, this protocol has limitations with the usage of only Meldrum's acid as a active methylene compound to afford the desired products in excellent yield and stoichiometric amount of toxic metal based catalysts.<sup>18–21</sup> Recently, Gu et al. reported the application of Yonemitsu reaction for the synthesis of 3-substituted indoles using indole, benzaldehyde and dimedone as active methylene compounds in the presence of *L*-proline as a homogeneous organocatalyst.<sup>22</sup> Recently, we reported RGO/ZnO nanocomposites as versatile heterogeneous catalysts for the synthesis of various 3-substituted indoles in water.<sup>23</sup> However, the design and development of very simple and efficient method for the synthesis of 3-substituted indoles via Yonemitsu type reaction remains a challenging task. In the continuation of our effort toward green chemistry,<sup>24–26</sup> herein we disclosed the synthesis of unusual rectangular thin sheets of hydromagnesite (RS-HM)

Received: March 23, 2015

Revised: May 23, 2015

Published: May 28, 2015

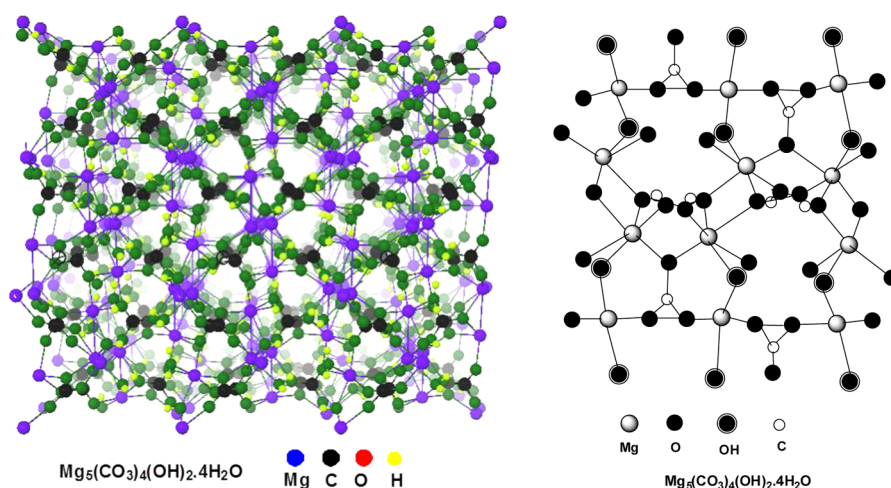


Figure 1. Three-dimensional structural model of hydromagnesite.

as a more efficient nanocatalyst than MgO for the synthesis 3-substituted indoles via Yonemitsu type reaction in water.

## RESULTS AND DISCUSSION

### Preparation and Characterization of RS-HM and MgO.

RS-HM was synthesized from readily available cheap starting materials using a conventional heating method and further calcined at 450 °C in the presence of air for 5 h to afford MgO. The synthesized materials were characterized by X-ray diffraction (XRD), scanning electronic microscopy (SEM), transmission electronic microscopy (TEM), Fourier transform infrared spectroscopy (FT-IR), Brunauer–Emmett–Teller (BET) surface area, thermal gravimetric analysis (TGA), etc. The powder X-ray diffraction (PXRD) pattern of RS-HM was indexed to have monoclinic symmetry (space group  $p2/c$ ) with refined lattice parameters of  $a = 10.1216(3)$ ,  $b = 8.9454(5)$ ,  $c = 8.3821(2)$  Å and  $\beta = 114.49$  °C (Figure 2). The crystallite size of RS-HM was calculated from the most intense plane (0 2 2) using the Debye–Scherrer formula and found to be 16 nm. All the reflections matched well with the reported data (JCPDS file no. 25-513) (Figure 2a).<sup>27</sup>

Thermal decomposition and the endothermic nature of RS-HM was studied by using a TG-DTA technique (see the

Supporting Information, Figure S1). Three distinct weight loss steps are observed in the temperature range of 100–170 °C (8.1%) attributed to the dehydration of crystalline water and second step is dehydroxylation process at 170–270 °C (12.6%). The third step is due to the evolution of CO<sub>2</sub> from the RS-HM at 280–480 °C (35.8%). The total weight loss in three steps is summed up to 56.5%, which is very close to the predicted theoretical weight loss of 56.7% for stoichiometric conversion of RS-HM to MgO.<sup>28</sup> The powder X-ray diffraction pattern of MgO was indexed to be cubic (NaCl type) and the crystallite size was found to be 10 nm. All the reflections in PXRD matched well with the reported data (JCPDS file no. 79-0612).<sup>29</sup> The presence of carbonates, hydroxides and crystalline water of RS-HM and formation of MgO were confirmed by FT-IR technique (see the Supporting Information, Figure S2).<sup>27</sup>

The surface morphologies of as-synthesized RS-HM and MgO were characterized from scanning electronic microscopy (SEM), as shown in Figure 3. The results revealed that the

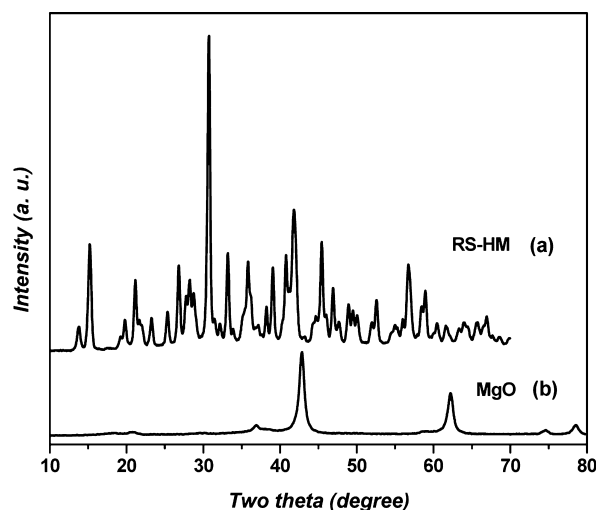


Figure 2. PXRD patterns of (a) RS-HM and (b) MgO.

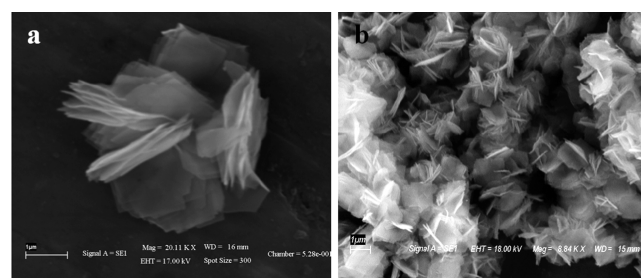
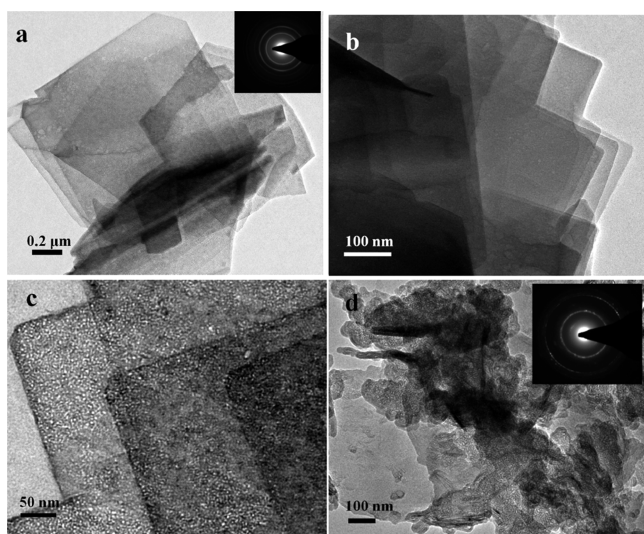


Figure 3. SEM images of (a) RS-HM and (b) MgO.

morphology of RS-HM exists as the rectangular sheets in a uniform manner and MgO exists as aggregated stacks (Figure 3). The internal morphologies of RS-HM and MgO were characterized from transmission electronic microscopy (TEM), as shown in Figure 4. It clearly shows that RS-HM exists as thin and transparent porous 2D sheets and MgO exists as porous distorted sheets. The RS-HM and MgO had a polycrystalline nature, as shown in inset of Figure 4a,d, respectively. Specific surface areas of the RS-HM and MgO were found to be 110 and 120 m<sup>2</sup>/g, respectively. The concentration of basic sites of RS-HM was calculated using titration method and found to be 23.8 mmol/g.



**Figure 4.** (a, b, c) Low to high magnified TEM images of RS-HM; (d) MgO; insets in panels a and d show SAED patterns of RS-HM and MgO, respectively.

**RS-HM Catalyst for Yonemitsu-Type Condensation.** The catalytic potential of RS-HM and MgO was explored for multicomponent synthesis of 3-substituted indoles via Yonemitsu-type condensation in water (Scheme 1). Initially, the optimization study was carried out for the model reaction among 2-bromobenzaldehyde, dimedone and indole in the presence of 10 mol % of RS-HM catalyst in various solvents at room temperature to 100 °C to afford 3-substituted indole **4a**, as shown in Table 1. The results revealed that the product **4a** was obtained in 70% yield along with side product xanthene **5a** in 25% yield in ethanol at 80 °C (entry 3, Table 1). In other organic solvents, the product **4a** was obtained in poor to moderate yields along with side product **5a** (entries 1–7, Table 1).

Interestingly, when water was used as a solvent, the rate of reaction increased drastically, leading to product **4a** in 90% yield selectively along with a trace amount of **5a** (Table 1, entry 8). Increase of catalyst loading has no effect in progress of the reaction to afford the product **4a** (entries 9 and 10). When temperature was either increased to 100 °C or decreased to 60 °C, the product **4a** was formed in 55–50% yield along with side product **5a** in 20–30% yield (entries 11 and 12). The progress of the reaction was slow under neat conditions, and the product **4a** was obtained in moderate yield with poor selectivity (entry 13). The model reaction was performed in the presence of nano MgO under optimized condition, the product **4a** was obtained in 70% yield along with side product **5a** in 20% yield (entry 14). The product **4a** was obtained in moderate yields 40–43% with poor selectivity in the presence of commercially

**Table 1. Optimization Study of RS-HM Catalysed Yonemitsu-Type Trimolecular Condensation<sup>a</sup>**

entry	catalyst (mol %)	solvent	temp (°C)	time (h)	yield of <b>4a</b> <sup>f</sup>	yield of <b>5a</b> <sup>f</sup>
1	RS-HM (10)	EtOH	rt	24	trace	trace
2	RS-HM (10)	EtOH <sup>c</sup>	60	6	40	30
3	RS-HM (10)	EtOH	80	3	70	25
4	RS-HM (10)	DMSO <sup>c</sup>	80	6	30	40
5	RS-HM (10)	DMF <sup>c</sup>	80	6	25	20
6	RS-HM (10)	MeOH <sup>c</sup>	65	10	50	20
7	RS-HM (10)	toluene <sup>c</sup>	80	6	40	40
8	RS-HM (10)	water	80	1	90	trace
9	RS-HM (20)	water	80	1	88	trace
10	RS-HM (30)	water	80	1	90	trace
11	RS-HM (10)	water	100	1	55	20
12	RS-HM (10)	water	60	1	50	30
13	RS-HM (10)	neat	80	6	45	35
14	MgO <sup>b</sup> (10)	water	80	4	70	20
15	MgO <sup>c</sup> (10)	water	80	6	40	45
16	MgO <sup>d</sup> (10)	water	80	6	43	47
17	RGO/ZnO	water	60	1	45	40

<sup>a</sup>Reaction conditions: 2-bromobenzaldehyde (1 mmol), dimedone (1 mmol) and indole (1 mmol), RS-HM catalyst (mol %), solvent 3 mL. <sup>b</sup>MgO obtained from calcination of RS-HM at 450 °C for 5 h in air. <sup>c,d</sup>Bulk MgO samples were purchased from Sigma-Aldrich and Alfa Aesar, respectively. <sup>e</sup>Unreacted Knoevenagel adduct and indole were recovered. <sup>f</sup>Isolated yield.

available bulk MgO (entries 14 and 15). We performed model reaction in the presence of RGO/ZnO catalyst, to compare the present results with our previous reported work.<sup>23</sup> The results reveal that RGO/ZnO catalyst gave almost similar results as compared with RS-HM for the model reaction at 60 °C in water to afford product **4a** in moderate yield (45%) along with side product **5a** (40%) (entries 12 and 17). But the yield of product **4a** was low in the presence of RGO/ZnO at 60 °C, when compared with the RS-HM at 80 °C (entries 17 and 8). Thus, the superior catalytic activity of RS-HM over MgO and RGO/ZnO catalysts was achieved in the presence of 10 mol % of RS-HM in water as the solvent at 80 °C temperature.

Encouraged by the above results, we studied the generality of method and comparative study of RS-HM with MgO catalyst for the synthesis of 3-substituted indole derivatives (**4a–4q**), as shown in Table 2. We performed experiments with aliphatic and aromatic aldehydes, active methylene compounds such as dimedone, and 1,3-cyclohexanedione and various indoles using RS-HM and MgO as catalysts under optimized conditions to afford the 3-substituted indole derivatives **4a–4q** (Table 2). The results indicate that almost all screened substrates afford the 3-substituted indoles in excellent yields with high selectivity in the presence of RS-HM catalyst, as shown in Table 2. But the reactions proceeded slowly in the presence of MgO catalyst to

**Scheme 1. RS-HM Catalyzed Yonemitsu-Type Trimolecular Condensation**

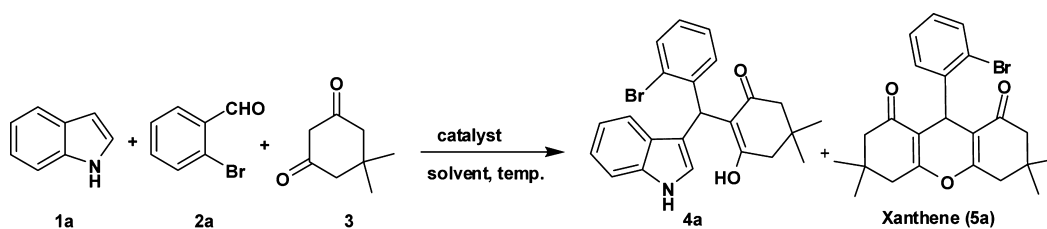
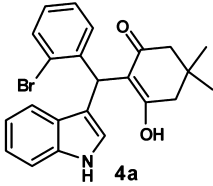
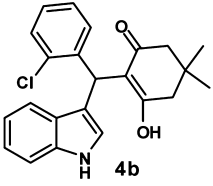
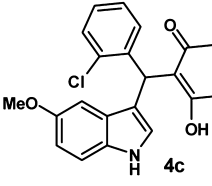
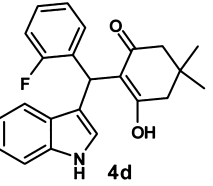
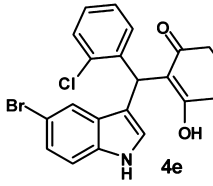
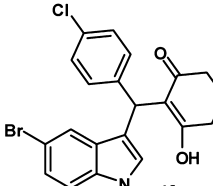
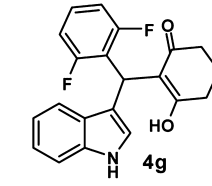
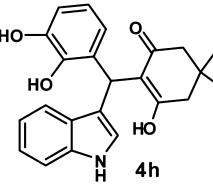
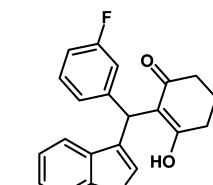
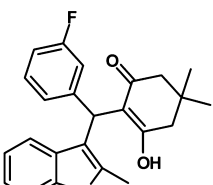
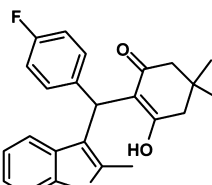
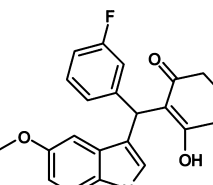
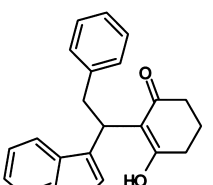
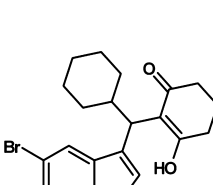
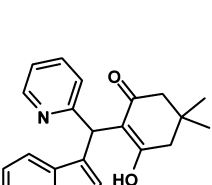
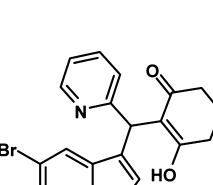
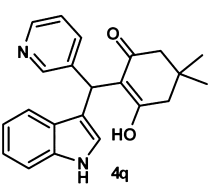




Table 2. RS-HM and MgO Catalyzed Synthesis of 3-Substituted Indoles

			
RS-HM: 90%, 1h MgO: 75%, 4h	RS-HM: 87%, 1h MgO: 77%, 3h	RS-HM: 91%, 1h MgO: 73%, 4h	RS-HM: 91%, 1h MgO: 73%, 4h
			
RS-HM: 85%, 2h MgO: 70%, 5h	RS-HM: 80%, 2h MgO: 65%, 4h	RS-HM: 87%, 1h MgO: 75%, 4h	RS-HM: 83%, 1h MgO: 70%, 3h
			
RS-HM: 86%, 1h MgO: 69%, 4h	RS-HM: 81%, 2h MgO: 60%, 5h	RS-HM: 83%, 2h MgO: 70%, 5h	RS-HM: 80%, 2h MgO: 63%, 5h
			
RS-HM: 90%, 2h MgO: 78%, 4h	RS-HM: 89%, 2h MgO: 76%, 3h	RS-HM: 83%, 1h MgO: 70%, 4h	RS-HM: 87%, 1h MgO: 75%, 5h
		RS-HM: 80%, 1h MgO: 73%, 3h	

afford products (4a–4q) in moderate to good yields along with the side product 5 (Table 2). It is noteworthy to mention here that the purification of final products was achieved by simple recrystallization from ethanol. The experimental observations reveal that the high catalytic activity of RS-HM over MgO is may be due to the presence of active Bronsted basic sites such as hydroxides ( $\text{OH}^-$ ), bicarbonates ( $\text{HCO}_3^-$ ) and Lewis acidic sites ( $\text{Mg}^{2+}$ ) and uncommon rectangular sheet morphology with high surface area ( $110 \text{ m}^2/\text{g}$ ) and its hydrophilic nature in water. Moreover, it is well-known that the organic reactions in

water has remarkable property and follows the “Breslow effect” to facilitate the reaction between substrates that are either soluble or insoluble in water.<sup>30</sup>

The plausible mechanism of RS-HM catalyst promoted Yonemitsu-type trimolecular condensation for the synthesis of 3-substituted indoles is depicted in Figure 5. The Lewis acidic sites ( $\text{Mg}^{2+}$ ) of RS-HM catalyst activate the carbonyl oxygen of aldehyde (2). The active Bronsted basic sites such as hydroxides ( $\text{OH}^-$ ) and bicarbonates ( $\text{HCO}_3^-$ ) of RS-HM abstract the proton from dimedone to promote the

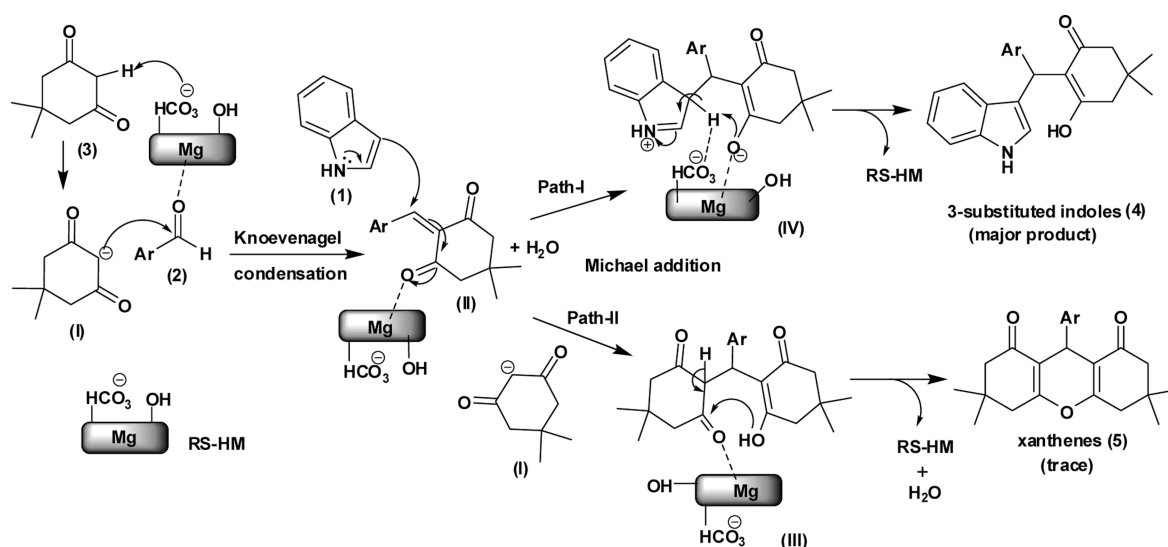


**Figure 5.** Plausible mechanism for the formation of 3-substituted indoles in the presence of RS-HM catalyst.

Knoevenagel condensation between the carbanion (I) and activated aldehyde (2) to afford the Knoevenagel adduct (II). The RS-HM can promote the Michael addition of indole (1) on the Knoevenagel adducts (II) to afford the 3-substituted indole (4), as shown in path I. However, there is a possibility of formation of side product (5) by the Michael addition of carbanion (I) on Knoevenagel adducts (II), as shown in path II (Figure 5).

**Recyclability Study of RS-HM Catalyst.** The recovery and reusability of the RS-HM catalyst was studied for the Yonemitsu-type condensation reaction among 2-bromobenzaldehyde, dimedone and indole under optimized reaction conditions, and the results are depicted in Figure 6. After the

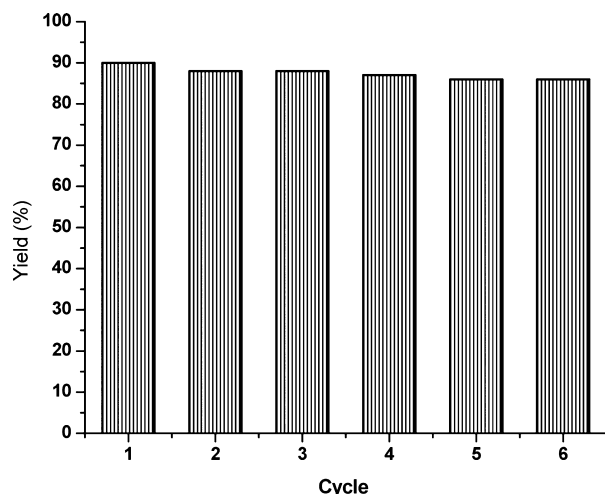


**Figure 6.** Recycling study of RS-HM catalyst for the synthesis of 3-substituted indole 4a.

experiment, the RS-HM catalyst was separated from the reaction mixture by simple centrifugation, and washed with ethanol for three times to remove adsorbed organic impurities from its surface. The recovered RS-HM catalyst was dried at 100 °C for 2 h under vacuum, and reused it for next runs under optimized reaction conditions. It was found that the RS-HM

catalyst could be reused for six times without significant loss in its catalytic activity, as depicted in Figure 6.

## CONCLUSION

In summary, we have described a simple method for the synthesis of the uncommon rectangular thin sheets morphology of hydromagnesite (RS-HM) with high surface area. The RS-HM catalyst showed excellent performance than MgO for the synthesis of 3-substituted indoles via Yonemitsu-type trimolecular condensation reaction. This method offers advantages such as environmentally benign (low *E*-factor (0.15) and high atom economy (AE) = 96%), mildness of the reaction conditions, ease to handle, widely applicable for various substrates, selectivity and excellent yields. The RS-HM catalyst was recycled for six times without loss in its catalytic activity.

## EXPERIMENTAL SECTION

**Typical Procedure for Synthesis of RS-HM Catalyst.** Mg(NO<sub>3</sub>)<sub>2</sub>·6H<sub>2</sub>O (3.7 g) was dissolved in 33 mL of urea solution (6 M) and mixed with 40 mL of ethylene glycol in a 100 mL round-bottomed flask. The reaction mixture was heated at 110 °C under continuous stirring (800 rpm) for 12 h. Afterward, the reaction mixture was cooled down to room temperature and centrifuged. The white precipitate (RS-HM) was collected and washed several times with deionized water followed by final washing with acetone and dried at 80 °C for 10 h in a vacuum oven. The RS-HM was thermally decomposed at 450 °C for 5 h in air to afford MgO.

**General Procedure for Synthesis of 3-Substituted Indoles (4a–4q).** A mixture of aldehyde (1.0 mmol), dimedone (1.0 mmol), indole (1.0 mmol) and RS-HM/MgO catalyst (10 mol %) in water (3.0 mL) was stirred at 80 °C until the reaction was completed (monitored by TLC). After completion, water was decanted, followed by the addition of ethanol to the reaction mixture. The solid catalyst was separated by centrifuge, and the crude product was purified by recrystallization from ethanol. All compounds were characterized by MP, IR, NMR and mass spectral data.

**2-((2-Bromophenyl)(1H-indol-3-yl)methyl)-3-hydroxy-5,5-dimethylcyclohex-2-enone (4a).** Pink solid. mp: 243–247 °C. IR ( $\nu_{\max}$ /cm<sup>-1</sup>, KBr): 3283, 3181, 2921, 2854, 1565, 1462, 1384, 1252, 1117, 1028. <sup>1</sup>H NMR (400 MHz, DMSO-*d*<sub>6</sub>):  $\delta$  10.95 (br s, 1H), 10.32 (br s, 1H), 7.27 (t, *J* = 7.6 Hz, 2H), 7.07 (d, *J* = 7.6 Hz, 3H), 7.03 (t, *J* = 7.6 Hz, 2H), 6.86 (s, 1H), 5.80 (s, 1H), 2.33–2.26 (m, 2H), 2.08 (s, 2H), 0.95 (s, 6H) ppm. <sup>13</sup>C NMR (100 MHz, DMSO-*d*<sub>6</sub>):  $\delta$  170.84, 141.20, 135.05, 132.71, 131.88, 128.61, 127.03, 126.00, 125.63, 123.02,

120.50, 114.91, 114.26, 113.51, 110.72, 43.20, 33.64, 31.41, 27.74 ppm. HRMS (ES) Calcd: 423.0834. Found: 424.0908 [M + H]<sup>+</sup> and 426.0892 [M + 2]<sup>+</sup>. Anal. Calcd for C<sub>23</sub>H<sub>22</sub>BrNO<sub>2</sub>: C, 65.10; H, 5.23; N, 3.30. Found: C, 65.21; H, 5.30; N, 3.39.

2-((2-Chlorophenyl)(1H-indol-3-yl)methyl)-3-hydroxy-5,5-dimethylcyclohex-2-enone (**4b**). Pink solid. mp: 207–210 °C. IR ( $\nu_{\max}/\text{cm}^{-1}$ , KBr): 3332, 3149, 2955, 2922, 1562, 1463, 1377, 1260, 1153, 1097. <sup>1</sup>H NMR (400 MHz, DMSO-*d*<sub>6</sub>):  $\delta$  10.72 (br s, 1H), 10.20 (br s, 1H), 7.27 (t, *J* = 8.3 Hz, 2H), 7.07 (d, *J* = 7.6 Hz, 1H), 7.04 (d, *J* = 7.6 Hz, 1H), 6.99 (d, *J* = 8.3 Hz, 1H), 6.95 (d, *J* = 8.3 Hz, 2H), 6.82 (s, 1H), 6.79 (t, *J* = 7.6, 1H), 5.85 (s, 1H), 2.35–2.09 (m, 4H), 0.96 (s, 6H) ppm. <sup>13</sup>C NMR (100 MHz, DMSO-*d*<sub>6</sub>):  $\delta$  147.21, 136.88, 133.22, 132.80, 129.00, 127.33, 125.97, 124.85, 121.20, 119.00, 118.62, 115.44, 115.14, 111.86, 34.37, 31.98, 28.65, 28.31 ppm. HRMS (ES) Calcd: 379.1339. Found: 380.1356 [M + H]<sup>+</sup> and 381.1342 [MH + 2]<sup>+</sup>. Anal. Calcd for C<sub>23</sub>H<sub>22</sub>ClNO<sub>2</sub>: C, 72.72; H, 5.84; N, 3.69. Found: C, 71.88; H, 5.61; N, 3.87.

2-((2-Chlorophenyl)(5-methoxy-1H-indol-3-yl)methyl)-3-hydroxy-5,5-dimethylcyclohex-2-enone (**4c**). Off white solid. mp: 201–204 °C. IR ( $\nu_{\max}/\text{cm}^{-1}$ , KBr): 3295, 3189, 2948, 1616, 1565, 1476, 1381, 1256, 1207, 1165, 1090, 1041, 924. <sup>1</sup>H NMR (400 MHz, DMSO-*d*<sub>6</sub>):  $\delta$  10.56 (br s, 1H), 10.19 (br s, 1H), 7.27 (d, *J* = 8.3 Hz), 7.18 (d, *J* = 9.1 Hz, 2H), 7.11 (d, *J* = 7.6 Hz, 1H), 7.06 (t, *J* = 7.6 Hz, 2H), 7.01 (t, *J* = 7.6 Hz, 2H), 6.76 (s, 1H), 5.79 (s, 1H), 3.53 (s, 3H), 2.34–2.30 (m, 2H), 2.08 (s, 2H), 0.96 (s, 6H) ppm. <sup>13</sup>C NMR (100 MHz, DMSO-*d*<sub>6</sub>):  $\delta$  196.07, 170.85, 153.38, 142.17, 133.22, 132.56, 132.14, 129.03, 127.40, 126.04, 125.50, 115.13, 112.49, 110.90, 101.22, 55.72, 50.75, 43.86, 34.45, 31.98, 28.59, 28.30 ppm. HRMS (ES) Calcd: 409.1445. Found: 410.1450 [M + H]<sup>+</sup> and 412.1449 [MH + 2]<sup>+</sup>. Anal. Calcd for C<sub>24</sub>H<sub>24</sub>ClNO<sub>3</sub>: C, 70.32; H, 5.90; 3.42. Found: C, 70.46; H, 5.24; N, 3.76.

2-((2-Fluorophenyl)(1H-indol-3-yl)methyl)-3-hydroxy-5,5-dimethylcyclohex-2-enone (**4d**). Off white solid. mp: 193–197 °C. IR ( $\nu_{\max}/\text{cm}^{-1}$ , KBr): 3867, 3741, 3617, 3346, 3105, 2960, 2352, 2315, 1699, 1643, 1561, 1484, 1384, 1264, 1223, 1157, 1099, 1029. <sup>1</sup>H NMR (400 MHz, DMSO-*d*<sub>6</sub>):  $\delta$  10.75 (br s, 1H), 10.31 (br s, 1H), 7.33 (d, *J* = 8.3 Hz, 1H), 7.14–6.99 (m, 5H), 6.92 (t, *J* = 7.6 Hz, 1H), 6.85 (t, *J* = 7.6 Hz, 2H), 5.96 (s, 1H), 2.39–2.33 (m, 2H), 2.12 (br s, 2H), 0.99 (s, 6H). <sup>13</sup>C NMR (100 MHz, DMSO-*d*<sub>6</sub>):  $\delta$  = 161.93, 159.52, 136.73, 132.07, 131.46, 127.30, 124.64, 123.26, 121.16, 118.90, 118.60, 115.63, 115.12, 114.71, 111.79, 32.01, 29.55, 28.32 ppm. HRMS (ES) Calcd: 363.1635. Found: 364.1625 [M + H]<sup>+</sup> and 366.1639 [MH + 2]<sup>+</sup>; Anal. Calcd for C<sub>23</sub>H<sub>22</sub>FNO<sub>2</sub>: C, 76.01; H, 6.10; N, 3.15. Found: C, 76.24; H, 6.09; N, 3.21.

2-((5-bromo-1H-indol-3-yl)(2-chlorophenyl)methyl)-3-hydroxy-5,5-dimethylcyclohex-2-enone (**4e**). Pink solid. mp: 192–195 °C. IR ( $\nu_{\max}/\text{cm}^{-1}$ , KBr): 3909, 3862, 3830, 3744, 3679, 3648, 3620, 3327, 2959, 2349, 2313, 1741, 1693, 1566, 1462, 1378, 1263, 1154, 1098, 1020. <sup>1</sup>H NMR (400 MHz, DMSO-*d*<sub>6</sub>):  $\delta$  10.76 (br s, 1H), 10.24 (br s, 1H), 7.50 (d, *J* = 7.6 Hz, 1H), 7.34 (d, *J* = 7.6 Hz, 1H), 7.15 (d, *J* = 7.6 Hz, 1H), 7.09 (t, *J* = 7.6 Hz, 1H), 7.04–6.99 (m, 3H), 6.84 (t, *J* = 7.6 Hz, 2H), 5.84 (s, 1H), 2.44–2.31 (m, 2H), 2.14 (br s, 2H), 1.04 (s, 6H) ppm. <sup>13</sup>C NMR (100 MHz, DMSO-*d*<sub>6</sub>):  $\delta$  195.99, 171.11, 143.89, 136.92, 133.09, 132.31, 127.73, 126.54, 124.08, 121.21, 119.02, 118.57, 115.77, 115.03, 111.88, 50.75, 43.83, 37.04, 31.94, 28.41 ppm. HRMS (ES) Calcd: 457.0444. Found: 458.0452 [M + H]<sup>+</sup> and 460.0449 [MH + 2]<sup>+</sup>. Anal. Calcd for C<sub>23</sub>H<sub>21</sub>BrClNO<sub>2</sub>: C, 60.21; H, 4.61; N, 3.05. Found: C, 60.30; H, 4.72; N, 3.13.

2-((2,6-Difluorophenyl)(1H-indol-3-yl)methyl)-3-hydroxy-5,5-dimethylcyclohex-2-enone (**4g**). Red solid. mp: 149–152 °C. IR ( $\nu_{\max}/\text{cm}^{-1}$ , KBr): 3410, 3346, 2959, 1641, 1586, 1464, 1423, 1377, 1257, 1223, 1179, 999. <sup>1</sup>H NMR (400 MHz, DMSO-*d*<sub>6</sub>):  $\delta$  10.90 (br s, 1H), 10.88 (br s, 1H), 7.34 (d, *J* = 7.6 Hz, 1H), 7.28 (t, *J* = 8.3 Hz, 2H), 7.14 (s, 1H), 7.07 (d, *J* = 8.3 Hz, 1H), 7.00 (d, *J* = 6.8 Hz, 1H), 6.90 (d, *J* = 6.8 Hz, 2H), 5.33 (s, 1H), 2.69–2.58 (m, 4H), 1.05 (s, 3H), 0.86 (s, 3H) ppm. <sup>13</sup>C NMR (100 MHz, DMSO-*d*<sub>6</sub>):  $\delta$  196.30, 164.29, 136.65, 128.83, 125.51, 123.96, 121.51, 121.20, 118.99, 118.58, 117.85, 112.77, 112.10, 50.63, 32.16, 29.20, 26.98, 24.02 ppm. HRMS (ES) Calcd: 381.1540. Found: 382.1538 [M + H]<sup>+</sup>. Anal. Calcd for C<sub>23</sub>H<sub>21</sub>F<sub>2</sub>NO<sub>2</sub>: C, 72.43, H, 5.55, N, 3.67. Found: C, 72.57, H, 5.72, N, 3.78.

2-((2,3-Dihydroxyphenyl)(1H-indol-3-yl)methyl)-3-hydroxy-5,5-dimethylcyclohex-2-enone (**4h**). Pink solid. mp: 259–263 °C. IR ( $\nu_{\max}/\text{cm}^{-1}$ , KBr): 3861, 3742, 3678, 3649, 3620, 3423, 3388, 2953, 2671, 2377, 2350, 2314, 1741, 1693, 1642, 1589, 1516, 1467, 1384, 1289, 1204, 1119, 1062. <sup>1</sup>H NMR (400 MHz, DMSO-*d*<sub>6</sub>):  $\delta$  10.77 (br s, 1H), 9.63 (s, 1H), 7.41 (d, *J* = 8.3 Hz, 1H), 7.25 (d, *J* = 7.6 Hz, 1H), 7.10 (s, 1H), 6.97 (t, *J* = 7.6 Hz, 1H), 6.87 (t, *J* = 7.6 Hz, 1H), 6.76 (t, *J* = 7.6 Hz, 1H), 6.66–6.62 (m, 2H), 5.1 (s, 1H), 2.62 (br s, 2H), 2.27–2.04 (m, 2H), 1.04 (s, 3H), 0.92 (s, 3H) ppm. <sup>13</sup>C NMR (100 MHz, DMSO-*d*<sub>6</sub>):  $\delta$  196.05, 164.15, 145.14, 137.81, 136.35, 126.80, 125.26, 124.31, 122.47, 120.70, 119.7, 119.30, 118.39, 118.32, 113.89, 111.83, 111.47, 50.28, 31.68, 28.78, 28.61, 26.79 ppm. HRMS (ES) Calcd: 377.1627. Found: 378.1635 [M + H]<sup>+</sup>. Anal. Calcd for C<sub>23</sub>H<sub>23</sub>NO<sub>4</sub>: C, 73.19; H, 6.14; N, 3.71. Found: C, 73.22; H, 6.09; N, 3.78.

2-((3-Fluorophenyl)(1H-indol-3-yl)methyl)-3-hydroxy-5,5-dimethylcyclohex-2-enone (**4i**). Red solid. mp: 159–163 °C; IR ( $\nu_{\max}/\text{cm}^{-1}$ , KBr): 3410, 3346, 2959, 1641, 1586, 1464, 1423, 1377, 1257, 1223, 1179, 999. <sup>1</sup>H NMR (400 MHz, DMSO-*d*<sub>6</sub>):  $\delta$  10.80 (br s, 1H), 10.57 (br s, 1H), 7.32 (d, *J* = 7.6 Hz, 1H), 7.18 (t, *J* = 8.3 Hz, 2H), 7.02 (d, *J* = 7.6 Hz, 1H), 6.96 (d, *J* = 7.6 Hz, 1H), 6.92 (s, 1H), 6.88–6.81 (m, 2H), 5.79 (s, 1H), 2.43 (br s, 2H), 2.14 (s, 2H), 0.98 (s, 6H) ppm. <sup>13</sup>C NMR (100 MHz, DMSO-*d*<sub>6</sub>):  $\delta$  190.71, 160.67, 147.98, 135.96, 129.05, 127.32, 124.17, 120.67, 118.46, 118.15, 116.25, 115.06, 114.58, 111.33, 111.75, 31.68, 27.94 ppm. HRMS (ES) Calcd: 363.1635. Found: 364.1638 [M + H]<sup>+</sup>. Anal. Calcd for C<sub>23</sub>H<sub>22</sub>FNO<sub>2</sub>: C, 76.01; H, 6.10; N, 3.85. Found: C, 76.24; H, 6.32; N, 3.62.

2-((3-Fluorophenyl)(2-methyl-1H-indol-3-yl)methyl)-3-hydroxy-5,5-dimethylcyclohex-2-enone (**4j**). Off white solid. mp: 175–179 °C; IR ( $\nu_{\max}/\text{cm}^{-1}$ , KBr): 3842, 3730, 3672, 3631, 3612, 3581, 3461, 3202, 2928, 2358, 2430, 2318, 1816, 1690, 1505, 1462, 1375, 1330, 1270, 1231, 1173, 1121, 1012. <sup>1</sup>H NMR (400 MHz, DMSO-*d*<sub>6</sub>):  $\delta$  = 10.61 (br s, 1H), 10.50 (br s, 1H), 7.21 (d, *J* = 8.3 Hz, 2H), 6.97 (d, *J* = 7.6 Hz, 1H), 6.90–6.83 (m, 3H), 6.68–6.65 (m, 2H), 5.73 (s, 1H), 3.60 (s, 3H), 2.38 (s, 2H), 2.13 (s, 2H), 0.98 (s, 6H). <sup>13</sup>C NMR (100 MHz, DMSO-*d*<sub>6</sub>):  $\delta$  = 163.13, 160.73, 152.78, 147.93, 147.87, 131.16, 129.16, 129.08, 127.62, 124.92, 124.13, 116.19, 114.96, 114.80, 114.59, 111.99, 111.76, 110.54, 100.55, 55.22, 34.85, 31.67, 27.95 ppm. HRMS (ES) Calcd: 377.1791. Found: 378.1782 [M + H]<sup>+</sup>. Anal. Calcd for C<sub>24</sub>H<sub>24</sub>FNO<sub>2</sub>: C, 76.37; H, 6.41; N, 3.71. Found: C, 76.59; H, 6.25; N, 3.98.

2-((1H-Indol-3-yl)-2-phenylethyl)-3-hydroxy-5,5-dimethylcyclohex-2-enone (**4m**). Off white solid. mp: 170–172 °C. IR ( $\nu_{\max}/\text{cm}^{-1}$ , KBr): 3413, 3057, 2955, 1573, 1476, 1414, 1378, 1254, 1148, 1026, 884, 797. <sup>1</sup>H NMR (400 MHz, DMSO-*d*<sub>6</sub>):  $\delta$  10.62 (s, 1H), 10.42 (br s, 1H), 7.48 (d, *J* = 8.3 Hz, 1H), 7.25 (d, *J* = 8.3 Hz, 1H), 7.17–7.15 (m, 5H), 7.09–7.05 (m, 1H), 6.96 (t, *J* = 7.6 Hz, 1H), 6.85 (t, *J* = 7.6 Hz, 1H), 4.71–4.73 (m, 1H), 3.51 (t, *J* = 12.5 Hz, 1H), 3.20 (dd, *J* = 12.9 Hz, *J* = 6.8 Hz, 1H), 2.08–2.02 (m, 4H), 0.72 (s, 6H) ppm. <sup>13</sup>C NMR (100 MHz, DMSO-*d*<sub>6</sub>):  $\delta$  141.84, 135.75, 128.74, 127.75, 127.24, 125.36, 122.51, 120.37, 118.81, 117.96, 117.77, 114.97, 111.03, 37.69, 31.36, 31.19, 27.80 ppm. HRMS (ES) Calcd: 359.1885. Found: 359.1898. Anal. Calcd for C<sub>24</sub>H<sub>25</sub>NO<sub>2</sub>: C, 80.19; H, 7.01; N, 3.90. Found: C, 80.38; H, 7.18; N, 4.01.

2-((5-Bromo-1H-indol-3-yl)(cyclohexyl)methyl)-3-hydroxycyclohex-2-enone (**4n**). White solid. mp: 242–246 °C. IR ( $\nu_{\max}/\text{cm}^{-1}$ , KBr): 3644, 2923, 1553, 1481, 1418, 1368, 1261, 1188, 1080, 975, 879. <sup>1</sup>H NMR (400 MHz, DMSO-*d*<sub>6</sub>):  $\delta$  10.85 (s, 1H), 10.44 (br s, 1H), 7.66 (s, 1H), 7.21 (d, *J* = 8.3 Hz, 1H), 7.20 (s, 1H), 7.05 (d, *J* = 9.1 Hz, 1H), 3.98 (d, *J* = 10.6 Hz, 1H), 2.25 (br s, 4H). 1.73–1.69 (m, 2H), 1.62–1.55 (m, 5H), 1.15–1.03 (m, 3H), 0.80–0.61 (m, 2H) ppm. <sup>13</sup>C NMR (100 MHz, DMSO-*d*<sub>6</sub>):  $\delta$  133.92, 130.32, 124.62, 122.51, 120.94, 117.26, 116.56, 112.99, 110.53, 38.31, 35.81, 32.46, 31.31, 26.38, 26.03, 25.86, 20.71 ppm. HRMS (ES) Calcd: 401.0990. Found: [M + H]<sup>+</sup> 402.0100. Anal. Calcd for C<sub>21</sub>H<sub>24</sub>BrNO<sub>2</sub>: C, 62.69; H, 6.01; N, 3.48. Found: C, 62.78; H, 6.20; N, 3.61.

2-((1H-Indol-3-yl)(pyridin-2-yl)methyl)-3-hydroxy-5,5-dimethylcyclohex-2-enone (**4o**). White solid. mp: 245–247 °C. IR ( $\nu_{\max}/\text{cm}^{-1}$ , KBr): 3398, 2954, 2872, 1704, 1634, 1555, 1513, 1412, 1362, 1296, 1260, 1177, 1088, 1047, 871, 808, 744. <sup>1</sup>H NMR (400 MHz, DMSO-



$d_6$ ):  $\delta$  14.84 (br s, 1H), 10.78 (s, 1H), 8.55–8.54 (m, 1H), 7.92 (t,  $J = 7.6$  Hz, 1H), 7.65 (d,  $J = 7.6$  Hz, 1H), 7.40 (t,  $J = 6.8$  Hz, 1H), 7.28 (d,  $J = 8.3$  Hz, 2H), 7.00 (t,  $J = 7.6$  Hz, 1H), 6.85 (t,  $J = 7.6$  Hz, 1H), 6.80 (s, 1H), 6.04 (s, 1H), 2.25–2.19 (m, 4H), 0.92 (s, 6H) ppm.  $^{13}\text{C}$  NMR (100 MHz, DMSO- $d_6$ ):  $\delta$  162.21, 146.89, 139.59, 136.36, 126.31, 123.88, 122.63, 121.08, 118.62, 118.31, 115.21, 114.18, 111.43, 37.82, 31.13, 27.86 ppm. HRMS (ES) Calcd: 346.1681. Found: 346.1700. Anal. Calcd for  $\text{C}_{22}\text{H}_{22}\text{N}_2\text{O}_2$ : C, 76.28; H, 6.40; N, 8.09. Found: C, 76.32; H, 6.62; N, 8.25.

2-((5-Bromo-1H-indol-3-yl)(yridine-2-yl)methyl)-3-hydroxy-5,5-dimethylcyclohex-2-enone (**4p**). White solid. mp: 248–250 °C. IR ( $\nu_{\text{max}}/\text{cm}^{-1}$ , KBr): 3438, 3198, 2919, 1589, 1476, 1422, 1365, 1253, 1112, 1013, 885, 751.  $^1\text{H}$  NMR (400 MHz, DMSO- $d_6$ ):  $\delta$  10.80 (s, 1H), 10.69 (br s, 1H), 8.30–8.25 (m, 2H), 7.46 (d,  $J = 8.3$  Hz, 1H), 7.33 (d,  $J = 8.3$  Hz, 1H), 7.17–7.14 (m, 1H), 7.01 (t,  $J = 7.6$  Hz, 1H), 6.91 (s, 1H), 6.85 (t,  $J = 7.6$  Hz, 1H), 5.80 (s, 1H), 2.26 (br s, 2H), 2.09 (br s, 2H), 0.97 (s, 6H) ppm.  $^{13}\text{C}$  NMR (100 MHz, DMSO- $d_6$ ):  $\delta$  161.82, 147.05, 139.75, 135.06, 128.15, 124.41, 123.93, 123.63, 122.87, 121.05, 115.31, 114.22, 113.57, 111.06, 37.60, 31.22, 27.87 ppm. HRMS (ES) Calcd: 424.0786. Found:  $[\text{M} + \text{H}]^+$  425.0792. Anal. Calcd for  $\text{C}_{22}\text{H}_{21}\text{BrN}_2\text{O}_2$ : C, 62.13; H, 4.98; N, 6.59. Found: C, 62.23; H, 5.20; N, 6.72.

2-((1H-Indol-3-yl)(pyridin-3-yl)methyl)-3-hydroxy-5,5-dimethylcyclohex-2-enone (**4q**). White solid. mp: 252–254 °C. IR ( $\nu_{\text{max}}/\text{cm}^{-1}$ , KBr): 3356, 2919, 1587, 1478, 1422, 1365, 1319, 1258, 1110, 882, 739, 694.  $^1\text{H}$  NMR (400 MHz, DMSO- $d_6$ ):  $\delta$  14.73 (br s, 1H), 11.01 (s, 1H), 8.57–8.56 (m, 1H), 7.93 (t,  $J = 7.6$  Hz, 1H), 7.65 (d,  $J = 7.6$  Hz, 1H), 7.44–7.40 (m, 2H), 7.26 (d,  $J = 8.3$  Hz, 1H), 7.11 (d,  $J = 8.3$  Hz, 1H), 6.84 (s, 1H), 6.00 (s, 1H), 2.29–2.19 (m, 4H), 0.91 (s, 6H) ppm.  $^{13}\text{C}$  NMR (100 MHz, DMSO- $d_6$ ):  $\delta$  149.50, 146.10, 140.08, 136.06, 135.63, 127.12, 124.22, 122.65, 120.70, 118.50, 118.17, 115.77, 114.72, 111.40, 32.91, 31.67, 31.23, 27.97 ppm. HRMS (ES) Calcd: 346.1681. Found: 346.1699. Anal. Calcd for  $\text{C}_{22}\text{H}_{22}\text{N}_2\text{O}_2$ : C, 76.28; H, 6.40; N, 8.09. Found: C, 76.42; H, 6.59; N, 8.18.

## ■ ASSOCIATED CONTENT

### ● Supporting Information

General remarks, *E*-factor and atom economy (AE) calculations for compound **4a**, TGA-DSC analysis of RS-HM, FT-IR of RS-HM and MgO and  $^1\text{H}$ ,  $^{13}\text{C}$  NMR spectra of 3-substituted indoles. The Supporting Information is available free of charge on the ACS Publications website at DOI: 10.1021/acssuschemeng.5b00236.

## ■ AUTHOR INFORMATION

### Corresponding Author

\*D. S. Rawat. Fax: 91-11-27667501. Tel: 91-11-27662683. E-mail: dsrawat@chemistry.du.ac.in.

### Notes

The authors declare no competing financial interest.

## ■ ACKNOWLEDGMENTS

D.S.R. thanks DU-DST PURSE grant and University of Delhi, Delhi, India for financial support. U.C.R. and V.S.P. are thankful to UGC for the award of a senior research fellowship (SRF) and UGC grant 41-202/2012 (SR) for junior research fellowship (JRF), respectively. We thank USIC-CIF, University of Delhi, for providing facilities to acquire analytical data.

## ■ REFERENCES

- (1) Sajjalal, P. R.; Sreepasad, T. S.; Samal, A. K.; Pradeep, T. Anisotropic nanomaterials: Structure, growth, assembly, and functions. *Nano Rev.* **2011**, *2*, 5883 DOI: 10.3402/nano.v2i0.5883.
- (2) Arico, A. S.; Bruce, P.; Scrosati, B.; Tarascon, J. M.; Schalkwijk, W. V. Nanostructured materials for advanced energy conversion and storage devices. *Nat. Mater.* **2005**, *4*, 366–377.

(3) Cuenya, B. R. Synthesis and catalytic properties of metal nanoparticles: Size, shape, support, composition, and oxidation state effects. *Thin Solid Films* **2010**, *518*, 3127–3150.

(4) Bell, A. T. The impact of nanoscience on heterogeneous catalysis. *Science* **2003**, *299*, 1688–1691.

(5) Polshettiwar, V.; Varma, R. S. Green chemistry by nanocatalysis. *Green Chem.* **2010**, *12*, 743–754.

(6) Giraud, R. J.; Williams, P. A.; Sehgal, A.; Ponnusamy, E.; Phillips, A. K.; Manley, J. B. Implementing green chemistry in chemical manufacturing: A survey report. *ACS Sustainable Chem. Eng.* **2014**, *2*, 2237–2242.

(7) Hattori, H. Heterogeneous basic catalysis. *Chem. Rev.* **1995**, *95*, 537–550.

(8) Selvamani, T.; Yagyu, T.; Kawasaki, S.; Mukhopadhyay, I. Easy and effective synthesis of micrometer-sized rectangular MgO sheets with very high catalytic activity. *Catal. Commun.* **2010**, *11*, 537–541.

(9) Debecker, D. P.; Gaigneaux, E. M.; Busca, G. Exploring, tuning, and exploiting the basicity of hydrotalcites for applications in heterogeneous catalysis. *Chem.—Eur. J.* **2009**, *15*, 3920–3935.

(10) Akao, M.; Marumo, F.; Iwai, S. The crystal structure of hydromagnesite. *Acta Crystallogr., Sect. B: Struct. Crystallogr. Cryst. Chem.* **1974**, *30*, 2670–2672.

(11) Tome, B.; Cuesta, J. M. L.; Gaudont, P.; Benhassaine, A.; Crespy, A. Fire resistance and mechanical properties of a huntite/hydromagnesite/antimony trioxide/decabromodiphenyl oxide filled PP-PE copolymer. *Polym. Degrad. Stab.* **1996**, *53*, 371–379.

(12) Atay, H. Y.; Celi, E. Use of Turkish huntite/hydromagnesite mineral in plastic materials as a flame retardant. *Polym. Compos.* **2010**, *31*, 1692–1700.

(13) Li, J.; Le, Y.; Dai, W. L.; Li, H.; Fan, K. Self-assembled  $\text{Mg}_5(\text{CO}_3)_4(\text{OH})_2 \cdot 4\text{H}_2\text{O}$  nanosheet as an effective catalyst in the Baeyer–Villiger oxidation of cyclohexanone. *Catal. Commun.* **2008**, *9*, 1334–1341.

(14) Kumar, A.; Iwatani, K.; Nishimura, S.; Takagaki, A.; Ebitani, K. Promotion effect of coexistent hydromagnesite in a highly active solid base hydrotalcite catalyst for transesterifications of glycols into cyclic carbonates. *Catal. Today* **2012**, *185*, 241–246.

(15) Rajesh, U. C.; Manohar, S.; Rawat, D. S. Hydromagnesite as an efficient recyclable heterogeneous solid base catalyst for the synthesis of flavanones, flavonols and 1,4-dihydropyridines in water. *Adv. Synth. Catal.* **2013**, *355*, 3170–3178.

(16) Oikawa, Y.; Hirasawa, H.; Yonemitsu, O. Meldrum's acid in organic synthesis: A convenient one-pot synthesis of ethylindolepropionate. *Tetrahedron Lett.* **1978**, *20*, 1759–1764.

(17) Sapi, J.; Laronze, J. Y. Indole based multicomponent reactions towards functionalized heterocycles. *ARKIVOC* **2004**, 208–222.

(18) Renzetti, A.; Boffa, E.; Colazzo, M.; Gerard, S.; Sapi, J.; Chan, T. H.; Nakazawa, H.; Villanie, C.; Fontana, A. Yonemitsu-type condensations catalyzed by proline and  $\text{Eu}(\text{OTf})_3$ . *RSC Adv.* **2014**, *4*, 47992–47999.

(19) Viola, A.; Ferrazzano, L.; Martelli, G.; Ancona, S.; Gentilucci, L.; Tolomelli, A. An improved microwave assisted protocol for Yonemitsu-type trimolecular condensation. *Tetrahedron* **2014**, *70*, 6781–6788.

(20) Epifano, F.; Genovese, S.; Rosati, O.; Tagliapietra, S.; Pelucchini, C.; Curini, M. Ytterbium triflate catalyzed synthesis of  $\beta$ -functionalized indole derivatives. *Tetrahedron Lett.* **2011**, *52*, 568–571.

(21) Gerard, S.; Renzetti, A.; Lefevre, B.; Fontana, A.; Maria, P.; Sapi, J. Multicomponent reactions studies: Yonemitsu-type trimolecular condensations promoted by Ti(IV) derivatives. *Tetrahedron* **2010**, *66*, 3065–3069.

(22) Li, M.; Taheri, A.; Liu, M.; Sun, S.; Gua, Y. Three-component reactions of aromatic aldehydes and two different nucleophiles and their leaving ability-determined downstream conversions of the products. *Adv. Synth. Catal.* **2014**, *356*, 537–556.

(23) Rajesh, U. C.; Wang, J.; Prescott, S.; Tsuzuki, T.; Rawat, D. S. RGO/ZnO nanocomposite: An efficient, sustainable, heterogeneous, amphiphilic catalyst for synthesis of 3-substituted indoles in water. *ACS Sustainable Chem. Eng.* **2015**, *3*, 9–18.

(24) Rajesh, U. C.; Kholiya, R.; Thakur, A.; Rawat, D. S. [TBA][Gly] ionic liquid promoted multi-component synthesis of 3-substituted indoles and indolyl-4H-chromenes. *Tetrahedron Lett.* **2015**, *56*, 1790–1793.

(25) Rajesh, U. C.; Divya; Rawat, D. S. Functionalized super-paramagnetic Fe<sub>3</sub>O<sub>4</sub> as an efficient quasi-homogeneous catalyst for multi-component reactions. *RSC Adv.* **2014**, *4*, 41323–41330.

(26) Rajesh, U. C.; Kholiya, R.; Pavan, V. S.; Rawat, D. S. Catalyst-free, ethylene glycol promoted one-pot three component synthesis of 3-amino alkylated indoles via Mannich-type reaction. *Tetrahedron Lett.* **2014**, *55*, 2977–2981.

(27) Janet, C. M.; Viswanathan, B.; Viswanath, R. P.; Varadarajan, T. K. Characterization and photoluminescence properties of MgO microtubes synthesized from hydromagnesite flowers. *J. Phys. Chem. C* **2007**, *111*, 10267–10272.

(28) Hollingbery, L. A.; Hull, T. R. The thermal decomposition of huntite and hydromagnesite - A review. *Thermochim. Acta* **2010**, *509*, 1–11.

(29) Li, W. C.; Lu, A.-H.; Weidenthaler, C.; Schuth, F. Hard-templating pathway to create mesoporous magnesium oxide. *Chem. Mater.* **2004**, *16*, 5676–5681.

(30) Gawande, M. B.; Bonifacio, V. D. B.; Luque, R.; Branco, P. S.; Varma, R. S. Benign by design: Catalyst-free in-water, on-water green chemical methodologies in organic synthesis. *Chem. Soc. Rev.* **2013**, *42*, 5522–5551.